JOURNAL OF SOLID STATE CHEMISTRY 31, 69–80 (1980)

Single-Crystal Neutron Diffraction Study of the Fast-Ion Conductor β-Ag_2S Between 186 and 325°C

R. J. CAVA,* F. REIDINGER,†‡ AND B. J. WUENSCH*

*Department of Materials Science and Engineering, Massachusetts Institute of Technology, Cambridge, Massachusetts 02139; †Chemistry Department, Brookhaven National Laboratory, Upton, New York 11973

Received August 2, 1978, in revised form February 19, 1979

Partial Fourier synthesis of the silver ion density in bcc β-Ag_2S at several temperatures reveals cation delocalization in bands along ⟨100⟩. This density may be analytically represented by use of higher-rank tensors, with partial occupancy of both octahedral and tetrahedral interstices below 200°C, but only tetrahedral occupancy at higher temperatures. R values range from 2.6 to 5.9%. The distribution of mobile ions differs greatly in α-AgI and β-Ag_2S, despite similar anion arrays, reflecting the different silver ion concentrations and characteristics of the bonding present in the respective low-temperature phases.

Introduction

Between a monoclinic to body-centered cubic transition at 177°C, and a subsequent transformation at 593°C to a face-centered cubic form (*1*), β-Ag_2S is an electronic as well as a cation-disordered fast-ion conductor. The ionic conductivity of β-Ag_2S, due solely to transport of silver ions, rises from about 3 to about 6 $ohm^{-1}\,cm^{-1}$ over the temperature range of stability of the phase (*2–6*). The activation energy for silver migration is approximately 0.1 eV. The electronic component of the conductivity is much higher (about 100 $ohm^{-1}\,cm^{-1}$ at 200°C). As with α-AgI, the prototype cation-disordered superionic conductor, the anions form a bcc framework in space group $Im3m$. The mobile silver ions are presumably disordered among interstices in the anion array, but at a concentration twice that of α-AgI. A detailed comparison of the cation distribution in the two compounds is thus of great interest.

Rahlfs, from an X-ray powder diffraction study (*7*), proposed that the four silver ions per Ag_2S cell were distributed with equal probability over the 42 combined sites of the octahedrally coordinated 6(*b*) $0\frac{11}{22}$, tetrahedrally coordinated 12(*d*) $\frac{1}{4}0\frac{1}{2}$, and triangularly coordinated 24(*h*) 0*xx* positions of $Im3m$. This proposal appeared from the same laboratory and in the same journal as a refinement of this model for α-AgI by Strock (*8*). The suggestion of a similar model for β-Ag_2S was undoubtedly influenced by Strock's results. The occupancies of the three sites in Ag_2S were subsequently modified by Lowenhaupt and Smith (*9*) on the basis of a single-crystal X-ray refinement to R = 12.6%. The highest occupancy per site was assigned to the octahedral 6(*b*) position, and the lowest to the 3-coordinated 24(*h*) site.

In a recent single-crystal neutron diffraction study of α-AgI (*10*), we showed that the scattering density in the three sites of

‡ Presently affiliated with the Department of Energy and Environment, Brookhaven National Laboratory.

0022-4596/80/010069-12$02.00/0

the Strock "random occupancy" model was indeed nonzero. The silver distribution could be described to significantly greater precision, however, by large anisotropic and anharmonic vibrations of silver ions occupying solely the tetrahedral 12(d) positions. The formalism for such a description has been developed only recently. The present study was undertaken to ascertain whether this model would be valid for β-Ag_2S as well. The twofold increase in Ag concentration and a more favorable ratio of cation/anion scattering lengths (0.61/0.285 as opposed to 0.61/0.52 for AgI) suggested that the neutron diffraction experiments would be even more sensitive to the details of the Ag distribution.

Low-Temperature Ag_2S

The low-temperature form of Ag_2S (acanthite) is monoclinic, space group $P2_1/c$, with $a = 4.231$ Å, $b = 6.930$ Å, $c = 9.526$ Å, $\beta = 125.48°$, and contains four Ag_2S per cell. The structure (*11*), shown in projection along the b axis in Fig. 1a, contains two independent Ag and one S which occupy the general position of the space group. The atomic arrangement is a superstructure based upon a slightly distorted body-centered cubic

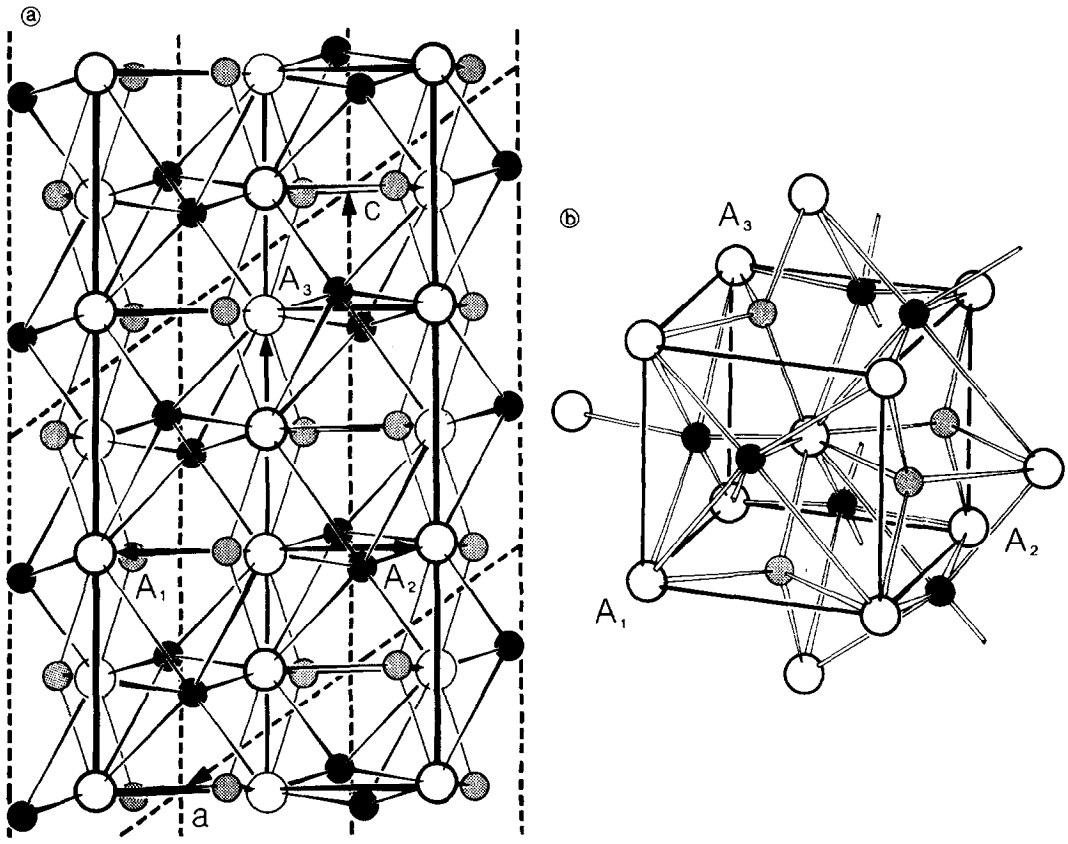

FIG. 1. Relation between the monoclinic structure of low-temperature Ag_2S and a pseudocubic body-centered subcell. (a) Projection of the low-temperature structure along b. The bold and light open circles represent S atoms located approximately at $+\frac{1}{4}b$ and $-\frac{1}{4}b$, respectively. The octahedrally coordinated Ag(1) and tetrahedrally coordinated Ag(2) ions are indicated by filled and shaded circles, respectively. (b) The atomic arrangement in a subcell. A sulfur atom has been placed at the origin.

array of sulfur atoms such that $[a, b, c] = [\frac{1}{2} -\frac{1}{2}-\frac{1}{2}/110/002][A_1, A_2, A_3]$. The subcell is pseudocubic, having $A_1 = A_2 = 4.887$ Å, $A_3 = 4.763$ Å, $\alpha_1 = 89.13°$, $\alpha_2 = 90.87°$, $\alpha_3 = 89.68°$. Two subcells are contained within the monoclinic supercell. The atomic configuration in a subcell is depicted in Fig. 1b. Although not required to do so by symmetry, the sulfur atoms are located very close to the nodes of the sublattice: If the origin of the subcell is placed at an S atom, the displacements of the other S atoms range from 0 to 0.19 Å (0.14 Å av).

The two types of Ag atoms occupy positions close to the octahedral and tetrahedral interstices, respectively, of an ideal bcc array. Displacements cause the bond distances to be irregular. Two S neighbors are present about the octahedral silver atom at 2.47 and 2.51 Å (2.49 Å av) plus four more distant at 3.03, 3.40, 3.47, and 3.83 Å (3.43 Å av). Though greatly distorted from a regular octahedron, the coordination is similar to the [2+4] coordination about this interstice in an ideal bcc array, for which the ratio of bond distances would be $2^{1/2}$ rather than the 1.38 observed for the averages. The tetrahedral silver has similar irregularities, the neighboring S atoms occurring at 2.52, 2.60, 2.70, and 2.99 Å (2.70 Å av). Examples for both linear coordination and [3+1] distorted tetrahedral coordination may be found for Ag in a number of other sulfides (*12*).

Experimental

Neutron diffraction experiments were carried out at the High-Flux Beam Reactor at Brookhaven National Laboratory on the four-circle diffractometer H6S4 with 1.0513-Å neutrons monochromated by (002) reflection from a Be single crystal. The sample was a crystal grown by Ohachi and co-workers (*13–15*) at 550°C in the stability field of the bcc β-form, but which had twinned upon cooling through the cubic–monoclinic transformation at 177°C. A cylinder 2.5 mm in diameter and 5.5 mm in length was cut from the upper portion of the crystal depicted in Fig. 6b of Ref. (*15*). As Ag_2S tends to lose sulfur by decomposition at temperatures above 200°C, the stoichiometry of the crystal was determined upon completion of its use in the diffraction experiments as was the stoichiometry of the adjacent portion of the crystal in its as-received state. The emf of the cell $Ag/AgI/Ag_{2+\delta}S/Pt$ was measured at 190°C and provided $\delta = 1.5$ and 6.0×10^{-4}, respectively, for the initial and final states of the crystal.[1] The silver excess is sufficiently small that, for present purposes, the ideal stoichiometric composition may be assumed.

The twinned crystal was mounted on a Cd-coated aluminum pin in an aluminum furnace (*16*) capable of a maximum temperature of 325°C. Upon heating toward the monoclinic–cubic transformation, the twinning of the crystal first increases, but then consolidates into a single crystal above the transformation temperature (*11*) because the monoclinic low-temperature sulfur array and its twinning relative to the cubic phase derive from minor local atomic displacements. Diffraction maxima from the transformed cubic phase were rather broad, necessitating that intensities be recorded with an ω-scan of constant length. A sufficiently large detector window intercepted all of the diffracted intensity over the angular range ($\sin\theta/\lambda \leq 0.58$ Å^{-1}) within which all reflections of significant intensity occurred.

The transformed single crystal of β-Ag_2S was studied at four temperatures in the sequence 200, 260, 325, and 186°C. The lattice constant and an orientation matrix were determined by least-squares techniques at each temperature under the program ORIENT (*17*). Three sets of symmetry-

[1] The measurements were kindly performed by Professor H. Schmalzried, Technische Universität, Hannover.

equivalent data were collected at each temperature under the program NXDAS2 (*17*). The agreement between equivalent reflections was within 1.5% after correction for absorption ($\mu_l = 1.25\ \text{cm}^{-1}$), and structure factors for 16 to 17 independent reflections were obtained by averaging. One or two $|F_{obs}| < \sigma$, but these were included in the data set. In comparison, only four structure factors were available in the powder-diffraction measurement of Rahlfs (*7*) and eight in the single-crystal X-ray study of Lowenhaupt and Smith (*9*).

Analysis of the structure was carried out at the Central Scientific Computer Facility at Brookhaven. We used Johnson's program ORJFLS (*18*), which allows incorporation and refinement of third- and fourth-rank thermal tensors (*19*). These tensors modify the conventional contribution to the structure factor for an atom with anisotropic harmonic thermal motion

$$f \exp(2\pi i h_j x_j - h_j h_k \beta_{jk}),$$

where f is the scattering length, h_j the Miller indices, x_j the atomic coordinates, and β_{jk} the second-order thermal parameters, by a factor accounting for anharmonic motion

$$[1 - 4\pi^3/3\ iH_{jkl}(\alpha)C_{jkl} + 2\pi^4/3\ H_{jklm}(\alpha)D_{jklm}],$$

where C_{jkl} and D_{jklm} are components of a third- and fourth-rank tensor, respectively; $H_{jkl}(\alpha)$ and $H_{jklm}(\alpha)$ are orthogonalized Hermite polynomials; and α is a variable which may be adjusted to minimize correlations between parameters of order p and $p+2$. The default value in ORJFLS, which takes α as the smaller of the values 0.45 or $(2\bar{U}_{ij})^{1/2}$, was found satisfactory. The Hermite polynomials assume simple form in the present structure because of high site symmetry. The only third-rank Hermite polynomial needed reduces to $H_{jkl} = h_j h_k h_l$. Explicit expressions for the required fourth-rank polynomials are listed in Table I.

The higher-order terms are the Fourier transform of a probability density which is a Taylor-like expansion about a Gaussian probability function. These orthogonalized polynomials represent an improvement over expansion of the structure factor in higher-order cumulants,

$$f \exp[i(2\pi h_j x_j - h_j h_k h_l C_{jkl}) - (h_j h_k \beta_{jk} - h_j h_k h_l h_m D_{jklm})],$$

introduced by Johnson in an earlier work (*20*) and previously regarded as the optimal formalism for the description of anharmonic motion (*21*). In either case one must use the expression "thermal" tensor cautiously as the formalism might equally well describe a probability density which is a positional rather than thermal disorder.

Results

Least-Squares Refinements

The experiments confirmed β-Ag_2S as cubic, space group $Im3m$, with the sulfur ions in a body-centered cubic array. The lattice constant (Table I) increased linearly with temperature with a linear thermal expansion coefficient of approximately $4.5 \times 10^{-5}\ °C^{-1}$.

Beginning with the data collected at 186°C, the structural model first examined was that obtained for α-AgI (*10*). Use of anisotropic harmonic temperature factors and third- and fourth-rank thermal parameters to describe the probability density of silver ions placed solely in the tetrahedral sites $12(d)\bar{4}0\frac{1}{2}$ resulted in a disagreement index[2] $R(F) = 4.2\%$. This was considered unsatisfactory relative to the

[2] The structure was refined on F^2_{obs}, minimizing the quantity $\sum w(F_o^2 - F_c^2)^2$, where the weights, w, are $[\sigma^2 + (0.01F_o^2)^2]^{-1}$, σ being the standard deviation due to counting statistics. $R(F) = \sum||F_o| - |F_c||/\sum|F_o|$, $R(F^2) = [\sum(F_o^2 - F_c^2)^2/\sum(F_o^2)^2]^{1/2}$, and the "weighted R," $R_w(F^2) = [\sum w(F_o^2 - F_c^2)^2/\sum w(F_o^2)^2]^{1/2}$.

TABLE I
LATTICE CONSTANTS AND THERMAL PARAMETERS FOR β-Ag_2S[a]

Temperature (°C)	186	200	260	325
Lattice, constant a (Å)	4.860(12)	4.862(4)	4.873(5)	4.889(9)
Scale factor	2.57(7)	2.50(13)	2.75(19)	2.91(22)
Extinction parameter, g, $\times 10^4$	5(3)	6(3)	15(7)	32(13)
Parameters[b] for sulfur in 2(a) 000				
B (Å^2)	4.27(16)	4.58(29)	5.91(47)	7.22(52)
$D_{1122}\times 10^6$	4.6(11)	7.4(15)	6(3)	10(3)
Parameters[c] for tetrahedral Ag in 12(d) $\frac{1}{4}\,0\frac{1}{2}$				
Total occupancy per cell	3.19(14)	3.34(19)	4.0	4.0
U_{11}	0.322(25)	0.326(30)	0.463(36)	0.451(31)
U_{22}	0.117(4)	0.116(5)	0.127(7)	0.138(7)
$C_{122}\times 10^4$	−4.54(38)	−3.72(43)	−2.8(8)	−2.3(7)
$D_{1111}\times 10^4$	—	—	−10.5(37)	−12.6(29)
$D_{1122}\times 10^4$	—	—	−0.21(12)	−0.32(12)
Parameters[d] for octahedral Ag in 6(b) $0\frac{11}{22}$				
Total occupancy per cell	0.81	0.66	0	0
U_{11}	0.146(17)	0.135(27)	—	—
$R(F)$ (%)	2.6	3.5	5.7	5.9
$R(F^2)$ (%)	1.7	2.5	2.9	3.0
$R_w(F^2)$ (%)	3.4	4.5	5.7	6.1

[a] Estimated standard deviations in parentheses. The temperature factor used is

$$\exp -2\pi^2(a^*)^2(h_ih_kU_{ik})[1-4\pi^3/3\; ih_ih_kh_iC_{jkl}+2\pi^4/3\; H_{jklm}(\alpha)D_{jklm}].$$

The fourth-order Hermite polynomials required are

$$H_{iiii}=h_i^4-\frac{6\alpha}{(2\pi)^2}\frac{a^2}{U_{ii}}+\frac{3\alpha^2}{(2\pi)^4}\frac{a^4}{U_{ii}^2},$$

$$H_{iikk}=h_i^2h_k^2-\frac{\alpha a^2}{(2\pi)^2}[h_k^2/U_{ii}+h_i^2/U_{kk}]+\frac{\alpha^2a^4}{(2\pi)^4}1/U_{ii}U_{kk}.$$

For S, $\alpha=0.3705$; for tetrahedral Ag, $\alpha=0.45$.

[b] For sulfur the temperature factor $T=\exp -B\sin^2\theta/\lambda$; $C_{jkl}\equiv 0$; $D_{1111}=D_{2222}=D_{3333}$, $D_{1122}=D_{1133}=D_{2233}$; all other $D_{jklm}\equiv 0$. The term D_{1111} was not significant and was omitted.

[c] For tetrahedral Ag, $T=\exp -2\pi^2[h^2U_{11}+(k^2+l^2)U_{22}](a^*)^2$; $C_{122}=-C_{133}$, all other $C_{jkl}\equiv 0$; $D_{2222}=D_{3333}$, $D_{1122}=D_{1133}$. Except for D_{1111} and D_{2233} other $D_{jklm}\equiv 0$.

[d] For Octahedral Ag, $T=\exp -2\pi^2[(h^2+k^2+l^2)U_{11}](a^*)^2$.

1.5% internal agreement between equivalent structure factors. Difference Fourier synthesis showed residual density in the octahedral interstice, 6(b)$0\frac{11}{22}$. The model was modified to include a fractional silver ion in this position, but the presence of fourth-order parameters for the tetrahedral silver caused the refinement to diverge. The best and final disagreement index, $R(F)=2.6\%$, was attained for a model which employed both tetrahedral and octahedral occupancy, employing only one third-order parameter for the tetrahedral Ag ions. Although involving the same number of parameters as the α-AgI-like model, the disagreement indices were improved by a factor of almost 2 ($R_w=3.4$ *vs* 6.6%). Of the 4 Ag ions per cell, 3.19(14) occupy tetrahedral interstices and 0.81(14) occupy octahedral sites. On the average, each tetrahedral site is occupied by 0.266(12) silver ion and each octahedral site by 0.135(23) ion.

For the data obtained at higher temperatures, occupation of the octahedral site lost statistical significance, the total occupancy of these positions being 0.4(6) at 325°C, for example, with correspondingly poor disagreement index of 8.3%. We attempted to describe the elongation of density along [100] at 325°C with the model proposed for α-AgI by Bührer and Hälg (*22*) in which the tetrahedral site is split to two locations $\frac{1}{2} \pm \Delta 0 \frac{1}{2}$. This resulted in an even poorer disagreement index of 9.3% although the number of parameters required remained the same. The model proposing occupancy of only tetrahedral 12(*d*) positions with higher-order thermal parameters produced significantly better refinements at 325 and 260°C of 5.9 and 5.7%, respectively. At temperatures below 200°C, therefore, both the tetrahedral and octahedral interstices are populated, but the occupancy of the latter site decreases with increasing temperature. Above 200°C placement of Ag ions solely in the tetrahedral sites provides an adequate description of the structure. The final parameters for the most satisfactory model at each of the four temperatures are presented in Table I. The squares of calculated and observed structure factors and their standard deviations, $\sigma(F_o^2)$, are provided in Table II.

Fourier Syntheses

Figure 2a presents a partial Fourier synthesis of the Ag ion density $\rho(xy0)$ in one face of the Ag_2S cell (contribution of S subtracted). This section contains the 6(*b*), 12(*d*), and 24(*h*) sites in the bcc S array. The Ag scattering density is confined to surprisingly uniform, continuous bands which connect tetrahedral and octahedral sites along [100]. Weak local maxima occur in the density at the tetrahedral and octahedral interstices. These maxima are significant features as their separation, $\frac{1}{4}a$, is twice the resolution of the Fourier map, $0.715\, d_{min} \approx \frac{1}{8}a$ (*23*). The maximum density of Fig. 2a is

TABLE II

COMPARISON OF SQUARES OF CALCULATED STRUCTURE FACTORS WITH SQUARES OF OBSERVED STRUCTURE FACTORS (CORRECTED FOR EXTINCTION) AND THEIR STANDARD DEVIATIONS

	186°C			200°C			260°C			325°C		
hkl	F_c^2	F_o^2	$\sigma(F_o^2)$	F_c^2	F_o^2	$\sigma(F_o^2)$	F_c^2	F_o^2	$\sigma(F_o^2)$	F_c^2	F_o^2	$\sigma(F_o^2)$
1 1 0	15.29	13.97	1.02	13.47	12.17	0.59	8.02	7.70	0.48	5.81	5.19	0.41
2 0 0	1208.80	1199.96	49.74	1185.71	1181.07	12.81	941.79	939.27	9.87	806.00	802.24	8.75
2 1 1	240.98	242.52	3.06	237.84	240.33	2.92	194.96	196.22	2.42	167.93	169.95	2.17
2 2 0	193.89	193.34	2.19	173.89	182.85	7.40	138.19	141.80	4.89	106.47	114.09	3.67
2 2 2	11.44	15.22	1.70	6.36	5.64	1.30	7.74	6.46	1.48	5.77	1.91	0.98
3 1 0	0.99	1.15	0.77	1.94	0.14	0.59	1.29	0.00	0.49	1.64	0.74	0.43
3 2 1	48.86	49.34	2.60	48.05	42.35	2.35	34.25	27.57	1.60	24.42	18.64	1.30
3 3 0	20.42	16.12	3.25	13.91	11.63	1.35	3.99	7.04	1.53	2.20	5.71	1.76
3 3 2	43.62	43.64	1.74	41.03	40.20	1.95	18.55	24.96	1.56	12.14	15.73	1.15
4 0 0	199.22	201.59	5.48	186.48	196.42	5.81	117.67	127.04	3.15	75.64	77.18	2.24
4 1 1	74.12	77.17	4.01	56.16	64.11	3.42	44.54	41.83	2.81	27.60	27.11	1.09
4 2 0	53.84	54.28	2.95	47.62	45.33	3.62	28.57	26.79	0.93	17.65	18.99	1.34
4 2 2	14.81	10.88	1.80	12.43	12.38	1.39	7.15	8.11	1.49	4.80	4.60	1.18
4 3 1	14.49	11.93	1.38	13.21	11.11	1.17	10.51	7.64	1.41	7.10	5.53	0.88
4 4 0	20.47	21.07	2.16	—	—	—	—	—	—	4.26	4.98	1.64
5 1 0	0.12	0.00	1.61	0.09	0.00	1.55	0.01	0.88	1.21	0.13	0.00	1.39
5 2 1	6.95	9.28	1.23	5.49	5.66	1.17	2.55	2.35	0.88	1.19	1.83	0.86

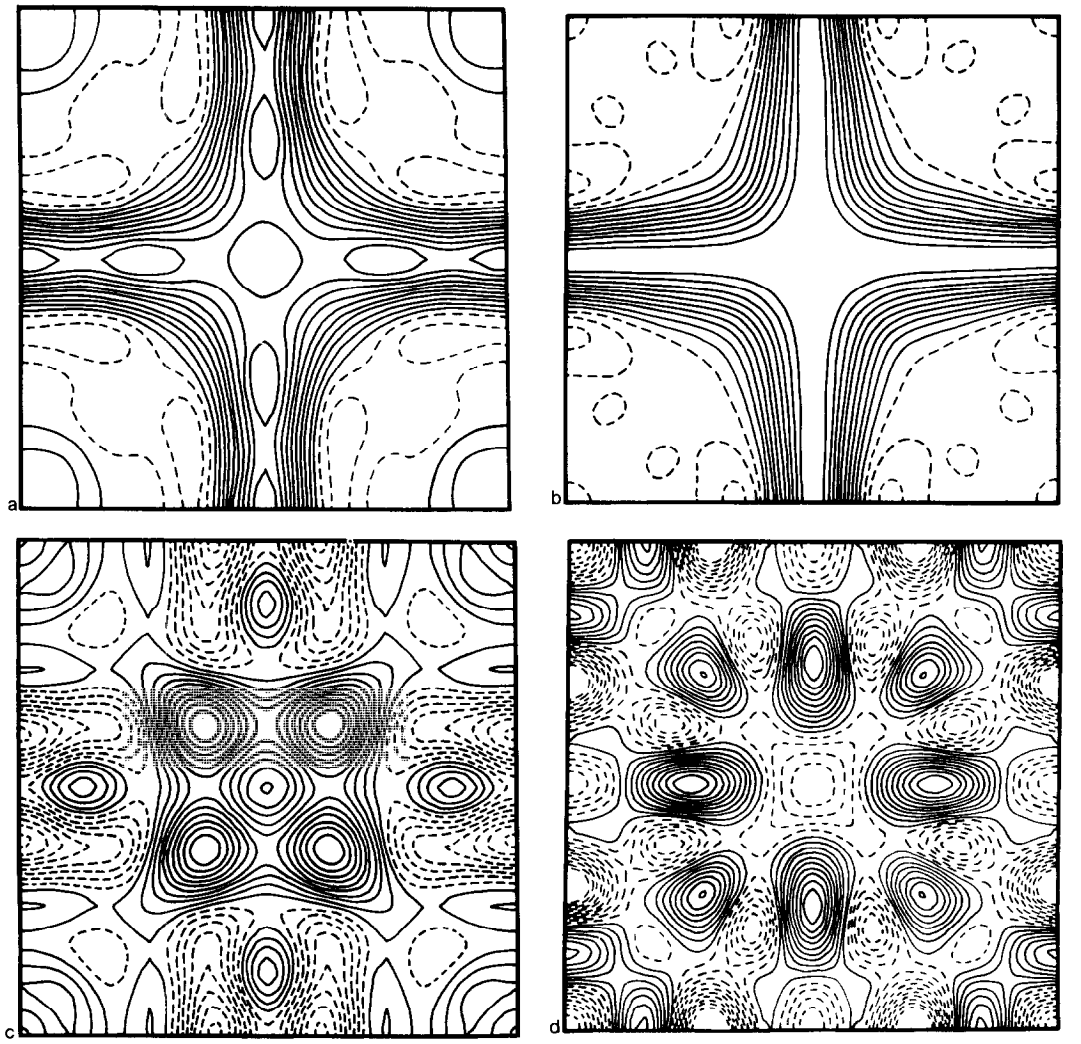

FIG. 2. Sections $\rho(xy0)$ of the scattering density in β-Ag_2S. (a) Partial Fourier synthesis of Ag scattering density at 186°C (contribution of S subtracted). Contour interval 0.0057×10^{-12} cm Å^{-3}, negative contours broken. (b) Partial Fourier synthesis of Ag scattering density at 325°C. Contour interval 0.0048×10^{12} cm Å^{-3}. (c) Distribution about the tetrahedral site of the portion of the Ag density which is accounted for by the third-rank thermal tensor at 186°C (subtracted are the contribution of S and also the contribution of the second-order harmonic thermal tensor for Ag). Contour interval 0.002×10^{-12} cm Å^{-3}. (d) Difference Fourier synthesis, $\rho_{obs}-\rho_{cal}$, for the final structural model for Ag_2S at 186°C. Contour interval 0.00031×10^{-12} cm Å^{-3} (note order-of magnitude increase in scale relative to preceding maps).

only 14.6% the maximum density (at the S atom) in a standard synthesis employing F_{obs}' as coefficients. Figure 2b represents the partial silver density, $\rho(xy0)$, at 325°C. (The maximum density is 18.6% of the maximum density, at S, in a normal synthesis based upon F_{obs}'.) The map reveals further delocalization of the Ag density, the weak maxima at the tetrahedral and octahedral sites at 186°C having disappeared in agreement with the results of the refinements.

The role of the third-rank tensor in describing the probability density of the mobile ions is illustrated in Fig. 2c. The maximum occurs at $\frac{3}{8}\frac{3}{8}0$, a position which is equidistant from all three S atoms in the triangular face shared between adjoining tetrahedra, and on the line connecting neighboring tetrahedral interstices. The density is 35% of that at the tetrahedral site—indicating, as in α-AgI, the importance of the higher-order terms in the description of the observed Ag probability distribution.

Figure 2d presents, at contour intervals an order of magnitude finer, a difference Fourier synthesis, $\rho_{obs}-\rho_{cal}$, for the structural model obtained for β-Ag_2S at 186°C. The maximum positive anomaly is located at the tetrahedral site and amounts to 5.4% of the maximum density of the partial Fourier synthesis (Fig. 2c; about half a contour interval). The maximum anomaly associated with the sulfur ion is 0.6% of the maximum sulfur density obtained in the F_{obs}' synthesis. A difference map for the model at 325°C is not presented. The silver probability densities at the octahedral and tetrahedral sites are described by the model to within 1.5%. The largest anomaly at 325°C is an overestimate, by about 5.6%, of the density between neighboring tetrahedral and octahedral sites. We find it remarkable that the higher-rank tensor formalism is able to describe, within 5%, a probability distribution which is as diffuse and continuous as that displayed in Fig. 2b.

Discussion

The Fourier syntheses and analytical structural models for β-Ag_2S indicate that the probability density of the mobile Ag ion is radically different from that in α-AgI, despite the same anion array. The silver in α-AgI between 147 and 300°C is localized at the tetrahedrally coordinated site with significant bridging density along ⟨110⟩. In β-Ag_2S, however, the silver is delocalized in bands along ⟨100⟩ and two different models are necessary to describe its distribution at temperatures between 186 and 325°C. The thermal vibration of S in Ag_2S is only about half that of I in α-AgI ($B_I = 8.5$ Å^2 at 200°C (*10*)), which is most likely a reflection of the increased interaction of Ag^+ with the divalent S^{2-} ions. Larger amplitudes would be anticipated if only the smaller mass of sulfur ($M_I/M_S \approx 4$) and the increased disorder of Ag were considered.

Above 200°C the Ag density in β-Ag_2S may be satisfactorily described by a tetrahedral Ag ion with strongly anisotropic second-order parameters ($U_{11}/U_{22} = 3.6$) and large higher-order parameters. As temperature decreases toward the phase transition at 177°C, the density at the octahedral site is most satisfactorily described by a partial atom. The ratio of the total occupancy of tetrahedral to octahedral sites is 5 : 1 at 200°C, 4 : 1 at 186°C, and is likely to approach 3 : 1 at the phase transition. It should be noted that, despite the change of models, the densities at the tetrahedral and octahedral sites remain equal. The ratio U_{11}/U_{22}, however, decreases to 2.6 at 186°C but remains significantly larger than the value of 1.9 found for Ag in α-AgI. (A value of 2.0 is expected for a particle which interacts via central forces with the surrounding atoms of the tetrahedral interstices in a bcc framework (*24*).) The third-order parameter C_{122} of Ag which describes the density near $\frac{3}{8}\frac{3}{8}0$ also behaves abnormally: It increases by about 50% as temperature changes from 325 to 186°C, while the corresponding term *decreases* by 25% for α-AgI for a similar decrease in temperature. The decreasing significance of the partial atom model for the description of the octahedral density, the decrease of the third-order parameter, and the increase of the ratio U_{11}/U_{22} all describe the increasing delocalization of Ag along ⟨100⟩ with increasing temperature.

It is noteworthy that the activation energy E measured for silver transport in α-AgI and

the ratio of the observed probability density at the saddle point, ρ_{sp}, and at the equilibrium site, ρ_0, are precisely related by the Boltzmann factor $\rho_{sp} = \rho_0 \exp -E/kT$. The results accordingly suggest a dynamic disorder involving severely anharmonic thermal motion. In contrast, while the activation energy for cation self-diffusion is about two times larger in β-Ag_2S than in α-AgI, the probability density is much more delocalized in the former, and is much larger at possible saddle points. The delocalization, therefore, cannot be completely due to the dynamics of the silver ion motion, but must include a large portion of positional disorder as well.

The significant difference between the probability densities of Ag in the fast-ion conducting phases of AgI and Ag_2S may be explained by two factors. The first is the difference in preferred coordination and bonding which is revealed in the respective low-temperature phases. Wurtzite-type β-AgI has silver ions which are tetrahedrally coordinated by I^- at equal distances (though this is not required by symmetry) of 2.82 Å (*10*). A tetrahedral interstice remains the equilibrium site in the cubic fast-ion conducting phase of α-AgI. The coordination and bond distances, 2.83 Å, remain basically unchanged through the phase transition, the only difference being distortion of the bond angles in the tetrahedron. The low-temperature form of Ag_2S contains both a [2+4] octahedrally coordinated cation with average bond distances of 2.49 and 3.43 Å, and a tetrahedrally coordinated cation with average bond length of 2.70 Å. These coordinations are also preserved through the phase transformation, as distances of 2.43 + 3.44 Å and 2.72 Å are observed about the ideal octahedral and tetrahedral interstices in the bcc S ion array. The presence of distorted bonding in the low-temperature Ag_2S structure, however, suggests that displacement of an individual ion within an interstice may be energetically favored. The observed distribution of density about each sort of interstice may thus contain positional disorder. The stable bonding in the low-temperature phases is thus reflected in the probability density of the mobile cations in the high-temperature phases. The distribution is not determined purely by the geometry of the anion array.

The second factor which distinguishes β-Ag_2S from α-AgI is the doubled concentration of the mobile cations. For a detailed description of this influence the local arrangements of Ag ions must be known, but the diffuse scattering experiments which can supply such insight have not yet been performed on Ag_2S. Interpretation of such measurements is difficult in any case, even for structures with but two-dimensional disorder (e.g., the β-aluminas). All that may presently be proposed, therefore, is a model which conforms to steric limitations.

Rickert (*25*) and Yokota (*26*) used the ionic radius of Ag and simple geometric arguments to construct "elementary regions" which could be occupied by one Ag ion only. Let us instead consider possible configurations of occupied interstices which take into account repulsive interactions between cations. The tetrahedral sites which surround each anion in a bcc array occupy the nodes of a cubo-octahedron (Fig. 3). Each node is shared by four cubo-octahedra which share square faces along ⟨100⟩ and hexagonal faces along ⟨111⟩. Nearest-neighbor tetrahedral sites are too close ($a2^{1/2}/4 = 1.71$ Å for Ag_2S) for any possibility of simultaneous occupancy, $2R$ for $(Ag^{IV})^+$ being 2.28 Å (*27*). Second-nearest tetrahedral sites are separated by $\frac{1}{2}a$ (2.43 Å in Ag_2S), barely twice the radius of an Ag ion, and occur along the diagonal of the square face of the cubo-octahedron. The third-nearest separations, $\frac{1}{2}a(\frac{3}{2})^{1/2}$ (2.98 Å) occur between alternate vertices of the hexagonal face.

As nearest-neighbor sites cannot be simultaneously occupied, the maximum possible filling of tetrahedral sites occurs

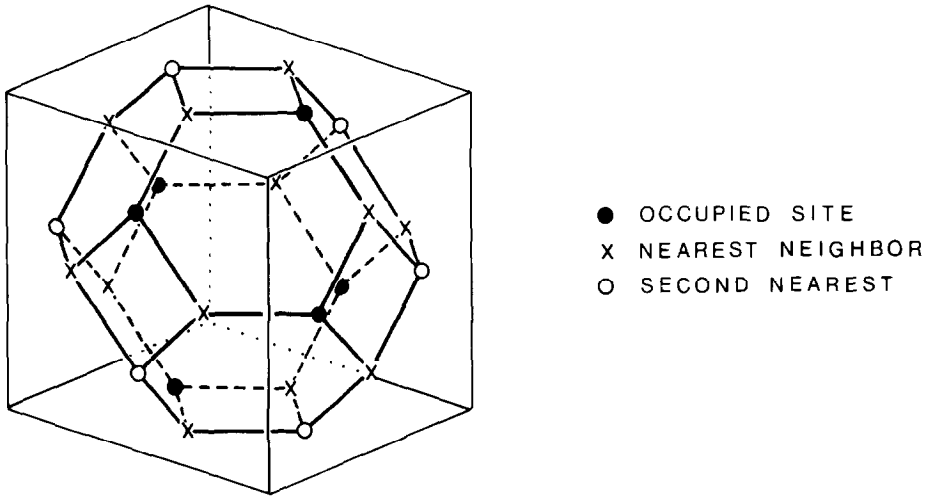

FIG. 3. The cubo-octahedron formed by the tetrahedral sites about each anion in a bcc array. The arrangement of occupied sites is one example of a disordered configuration in which both nearest and second-nearest sites are vacant, and which has the composition $Ag_{1.5}X$.

when alternate tetrahedral sites are occupied by Ag ions. This configuration is fully ordered, and has cell content Ag_6X_2. Ions occupy three of the six vertices of the hexagonal face and are separated by the third-nearest neighbor separation; the two occupied vertices of the square are separated by the second-nearest neighbor distance along its diagonal. A compound with this cation concentration cannot conduct by uncorrelated jumps as no vacancies are accessible.

Next consider a configuration in which both nearest and second-nearest sites are vacant. Relative to the preceding filled structure, this requires removal of one of the two ions from the square face of the cubo-octahedron, leaving only 6 of the 24 nodes occupied. The structure can be highly disordered as one, two, or three vertices of the hexagonal faces may be filled. The cell content of this configuration is Ag_3X_2 which, interestingly, is the concentration in Ag_3SI, a fast-ion conducting compound in the system AgI–Ag_2S (*28*). One possible disordered configuration is shown in Fig. 3. Isolated jumps are possible for every ion in this configuration as every ion is adjoined by at least one vacancy which is only a third-nearest neighbor to another occupied site. However, for the majority of jumps, cooperative motion will occur if simultaneous occupancy of second-nearest sites is to be avoided.

Let us now compare Ag_2S and AgI with the $Ag_{1.5}X$ composition described above. The cation concentration of AgI may be derived by removing one further Ag ion per cell (two per cubo-octahedron) thus creating additional accessible vacancies. Independent jumps appear favored for this composition. This view is confirmed by the molecular dynamics calculation of Vashishta and Rahman (*29*), who further show that jumps into second- and third-nearest sites are of significance.

To derive the structure of Ag_2S, two additional Ag ions must, on average, be added to each cubo-octadedron. If these are added to tetrahedral sites two square faces acquire second-nearest neighbors along the square diagonal regardless of the particular configuration assumed for $Ag_{1.5}X$. Another possibility would be placement of the addi-

tional ions in octahedral sites (the center of the square faces). As every square face already contains one ion in the $Ag_{1.5}X$ composition, occupation of an octahedral site must require displacement of this ion to a new tetrahedral location which will always have a second-nearest neighbor. Therefore two second-nearest neighbor ⟨100⟩ dimers must also be created per cubo-octahedron if octahedral sites are occupied.

The latter possibility leads to an occupancy ratio between tetrahedral and octahedral sites of 3:1, which is essentially that estimated by extrapolation of the present results to the temperature of the phase transformation. The Ag–S interaction evident in the bonding characteristics of the low-temperature phase apparently favors this arrangement, but only by a slight margin, because with increasing temperature the octahedral site loses its character as an equilibrium site and it is mainly the Ag–Ag interaction which determines the Ag probability density.

These considerations favor the caterpillar mechanism proposed by Yokota (*26*) and Okazaki (*4*) as a conduction mechamism. The collinear arrangements may, however, be frequently restricted to two ions, thus approaching an interstitialcy mechanism. Unlike α-AgI, the cation concentration of β-Ag_2S requires that at least one such ⟨100⟩ dimer be present per cell, regardless of whether only tetrahedral or a combination of tetrahedral and octahedral sites are occupied. A vacancy mechanism, as proposed by Rickert (*3*), seems unlikely, mainly because the repulsive Ag–Ag interaction restricts the accessibility and therefore the mobility of a vacancy.

Conclusions

The first single-crystal neutron diffraction study of the fast-ion conducting phase of Ag_2S shows that although the anion frameworks in α-AgI and β-Ag_2S are the same, the distribution of the mobile ions differs markedly because of different cation concentrations and bonding characteristics with the anions. Unlike α-AgI, where a jump-like diffusion between well-defined sites is suggested by the structural study, the fast-ion conducting phase of Ag_2S exhibits significant positional disorder of the silver ions and manifestations of significant cation–cation interactions.

Acknowledgments

This research was carried out at Brookhaven National Laboratory under contract with the U.S. Department of Energy and supported, in part, by its Division of Physical Research. Dr. T. Ohachi kindly provided the Ag_2S crystal used for measurement and Dr. J. S. White, U.S. National Museum, provided mineralogical specimens for preliminary study. To Professor H. Schmalzried, Hannover, we are indebted for the electrochemical determination of the stoichiometry of our specimens. Professor D. K. Smith kindly provided a preprint of his X-ray diffraction study.

References

1. B. J. SKINNER, *Econ. Geol.* **61**, 1 (1966).
2. R. ALLEN AND W. MOORE, *J. Phys. Chem.* **63**, 223 (1954).
3. H. RICKERT, *Z. Phys. Chem. N.F.* **23**, 355 (1960).
4. H. OKAZAKI, *J. Phys. Soc. Japan* **23**, 355 (1967).
5. I. BARTKOWICZ AND S. MROWEC, *Phys. Status Solidi B* **49**, 101 (1972).
6. T. OHACHI, Ph.D. thesis, Doshisha University, Kyoto (1974).
7. P. RAHLFS, *Z. Phys. Chem. Abt. B* **31**, 157 (1936).
8. L. W. STROCK, *Z. Phys. Chem. Abt. B* **25**, 411 (1934); **31**, 132 (1936).
9. D. E. LOWENHAUPT AND D. K. SMITH, "Program and Abstracts, Summer Meeting, American Crystallographic Association, Pennsylvania State University, August 18–23, 1974."
10. R. J. CAVA, F. REIDINGER, AND B. J. WUENSCH, *Solid State Commun.* **24**, 411 (1977).
11. R. SADANAGA AND S. SUENO, *Miner. J. Japan* **5**, 124 (1967).
12. W. NOWACKI, *Schweiz. Mineral. Petrogr. Mitt.* **49**, 109 (1969).
13. T. OHACHI, T. YAMAMOTO, AND I. TANIGUCHI, *J. Cryst. Growth* **24**, 576 (1974).
14. T. OHACHI AND I. TANIGUCHI, *J. Cryst. Growth* **40**, 109 (1977).

15. T. OHACHI AND B. R. PAMPLIN, *J. Cryst. Growth*, **42**, 592 (1977).
16. F. J. HOLLANDER, D. SEMMINGSEN, AND T. F. KOETZLE, to be published.
17. R. K. MCMULLAN AND (in part) L. C. ANDREWS, T. F. KOETZLE, F. REIDINGER, R. THOMAS, AND G. J. B. WILLIAMS, "NXDAS2 Neutron and X-ray Data Acquisition Systems," Brookhaven National Laboratory, unpublished.
18. C. K. JOHNSON, Oak Ridge National Laboratory, Oak Ridge, Tenn., unpublished.
19. C. K. JOHNSON AND H. A. LEVY, "International Tables for X-ray Crystallography," Vol. 4, Kynoch Press, Birmingham (1974).
20. C. K. JOHNSON, *Acta Crystallogr. Sect. A* **25**, 187 (1969).
21. C. SCHERINGER, *Acta Crystallogr. Sect. A* **33**, 879 (1977).
22. W. BÜHRER AND W. HÄLG, *Helv. Phys. Acta.* **47**, 27 (1974).
23. R. W. JAMES, *Acta Crystallogr.* **1**, 132 (1948).
24. F. REIDINGER, J. J. REILLY, AND R. W. STOENNER, to be published.
25. H. RICKERT, *Z. Phys. Chem. N. F.* **24**, 418 (1960).
26. I. YOKOTA, *J. Phys. Soc. Japan* **21**, 420 (1966).
27. R. D. SHANNON, *Acta Crystallogr. Sect. A* **32**, 751 (1976).
28. B. REUTER AND K. HARDEL, *Z. Anorg. Allg. Chem.* **340**, 158 (1965).
29. P. VASHISHTA AND A. RAHMAN, *Phys. Rev. Lett.* **40**, 1337 (1978).